Out-of-plane scattering from vertically asymmetric photonic crystal slab waveguides with in-plane disorder

Juraj Topolancik,[1,2,*] Frank Vollmer,[1,*] Rob Ilic,[3,*] and Michael Crescimanno[4]

[1]*Rowland Institute at Harvard, Harvard University, Cambridge, MA 02142, USA*
[2]*Department of Electrical and Computer Engineering, Northeastern University, Boston, MA 02115, USA*
[3]*Cornell NanoScale Facility, Department of Applied Physics and Field of Biophysics, Cornell University, Ithaca, NY 14853, USA*
[4]*Department of Physics and Astronomy, Youngstown State University, Youngstown, OH 44555, USA*
**jtopolan@ece.neu.edu, vollmer@rowland.harvard.edu, rob@cnf.cornell.edu*

Abstract: We characterize optical wave propagation along line defects in two-dimensional arrays of air-holes in free-standing silicon slabs. The fabricated waveguides contain random variations in orientation of the photonic lattice elements which perturb the in-plane translational symmetry. The vertical slab symmetry is also broken by a tilt of the etched sidewalls. We discuss how these lattice imperfections affect out-of-plane scattering losses and introduce a mechanism for high-Q cavity excitation related to polarization mixing.

OCIS codes: (230.5298) Photonic crystals; (230.5750) Resonators; (130.5296) Photonic crystal waveguides; (230.1350) Backscattering; (260.5740) Resonance.

References and links

1. J. D. Joannopoulos, S. G. Johnson, J. N. Winn, and R. D. Meade, *Photonic Crystal–Molding the Flow of Light* (Princeton University Press, 2008).
2. K. Inoue, and K. Ohtaka, eds., *Photonic Crystals–Physics, Fabrication and Applications* (Springer, 2003).
3. M. Notomi, T. Tanabe, A. Shinya, E. Kuramochi, H. Taniyama, S. Mitsugi, and M. Morita, "Nonlinear and adiabatic control of high-Q photonic crystal nanocavities," Opt. Express **15**(26), 17458–17481 (2007).
4. T. Uesugi, B. S. Song, T. Asano, and S. Noda, "Investigation of optical nonlinearities in an ultra-high-Q Si nanocavity in a two-dimensional photonic crystal slab," Opt. Express **14**(1), 377–386 (2006).
5. M. Soljacić, and J. D. Joannopoulos, "Enhancement of nonlinear effects using photonic crystals," Nat. Mater. **3**(4), 211–219 (2004).
6. T. Yoshie, A. Scherer, J. Hendrickson, G. Khitrova, H. M. Gibbs, G. Rupper, C. Ell, O. B. Shchekin, and D. G. Deppe, "Vacuum Rabi splitting with a single quantum dot in a photonic crystal nanocavity," Nature **432**(7014), 200–203 (2004).
7. D. Englund, D. Fattal, E. Waks, G. Solomon, B. Zhang, T. Nakaoka, Y. Arakawa, Y. Yamamoto, and J. Vucković, "Controlling the spontaneous emission rate of single quantum dots in a two-dimensional photonic crystal," Phys. Rev. Lett. **95**(1), 013904 (2005).
8. O. Painter, R. K. Lee, A. Scherer, A. Yariv, J. D. O'Brien, P. D. Dapkus, and I. Kim I, "Two-dimensional photonic band-Gap defect mode laser," Science **284**(5421), 1819–1821 (1999).
9. K. Hennessy, A. Badolato, M. Winger, D. Gerace, M. Atatüre, S. Gulde, S. Fält, E. L. Hu, and A. Imamoğlu, "Quantum nature of a strongly coupled single quantum dot-cavity system," Nature **445**(7130), 896–899 (2007).
10. S. Noda, A. Chutinan, and M. Imada, "Trapping and emission of photons by a single defect in a photonic bandgap structure," Nature **407**(6804), 608–610 (2000).
11. T. Tanabe, M. Notomi, S. Mitsugi, A. Shinya, and E. Kuramochi, "All-optical switches on a silicon chip realized using photonic crystal nanocavities," Appl. Phys. Lett. **87**(15), 151112 (2005).
12. M. Belotti, J. F. Galisteo Lòpez, S. De Angelis, M. Galli, I. Maksymov, L. C. Andreani, D. Peyrade, and Y. Chen, "All-optical switching in 2D silicon photonic crystals with low loss waveguides and optical cavities," Opt. Express **16**(15), 11624–11636 (2008).
13. D. O'Brien, A. Gomez-Iglesias, M.-D. Settle, A. Micheli, M. Salib, and T. F. Krauss, "Tunable optical delay using photonic crystal heterostructure nanocavities," Phys. Rev. B **76**, 1–4 (2007).
14. M. R. Lee, and P. M. Fauchet, "Two-dimensional silicon photonic crystal based biosensing platform for protein detection," Opt. Express **15**(8), 4530–4535 (2007).
15. D. Gerace, and L. C. Andreani, "Disorder-induced losses in photonic crystal waveguides with line defects," Opt. Lett. **29**(16), 1897–1899 (2004).

#109000 - $15.00 USD Received 20 Mar 2009; revised 17 Jun 2009; accepted 30 Jun 2009; published 8 Jul 2009

16. S. G. Johnson, M. L. Povinelli, M. Soljačić, A. Karalis, S. Jacobs, and J. D. Joannopoulos, "Roughness losses and volume-current methods in photonic-crystal waveguides," Appl. Phys. B **81**(2-3), 283–293 (2005).
17. S. Hughes, L. Ramunno, J. F. Young, and J. E. Sipe, "Extrinsic optical scattering loss in photonic crystal waveguides: role of fabrication disorder and photon group velocity," Phys. Rev. Lett. **94**(3), 033903 (2005).
18. N. Le Thomas, V. Zabelin, R. Houdré, M. V. Kotlyer, and T. F. Krauss, "Influence of residual disorder on the anti-crossing of Bloch modes probed in *k*-space," Phys. Rev. B **78**(12), 125301 (2008).
19. R. Ferrini, D. Leuenberger, R. Houdré, H. Benisty, M. Kamp, and A. Forchel, "Disorder-induced losses in planar photonic crystals," Opt. Lett. **31**(10), 1426–1428 (2006).
20. S. Mookherjea, J. S. Park, S.-H. Yang, and P. R. Bandaru, "Localization in silicon nanophotonic slow-light waveguides," Nat. Photonics **2**(2), 90–93 (2008).
21. Y. Lahini, A. Avidan, F. Pozzi, M. Sorel, R. Morandotti, D. N. Christodoulides, and Y. Silberberg, "Anderson localization and nonlinearity in one-dimensional disordered photonic lattices," Phys. Rev. Lett. **100**(1), 013906 (2008).
22. J. Topolancik, B. Ilic, and F. Vollmer, "Experimental observation of strong photon localization in disordered photonic crystal waveguides," Phys. Rev. Lett. **99**(25), 253901 (2007).
23. N. Le Thomas, V. Zabelin, R. Houdré, M. V. Kotlyar, and T. F. Krauss, "Influence of residual disorder on the anticrossing of Bloch modes probed in k space," Phys. Rev. B **78**(12), 125301 (2008).
24. Y. Tanaka, T. Asano, Y. Akahane, B. S. Song, and S. Noda, "Theoretical investigation of a two-dimensional photonic crystal slab with truncated cone air holes," Appl. Phys. Lett. **82**(11), 1661–1663 (2003).
25. J. Canning, N. Skivesen, M. Kristensen, L. H. Frandsen, A. Lavrinenko, C. Martelli, and A. Tetu, "Mapping the broadband polarization properties of linear 2D SOI photonic crystal waveguides," Opt. Express **15**(23), 15603–15614 (2007).
26. E. Dulkeith, S. J. McNab, and Y. A. Vlasov, "Mapping the optical properties of slab-type two-dimensional photonic crystal waveguides," Phys. Rev. B **72**(11), 115102 (2005).
27. J. Topolancik, F. Vollmer, and B. Ilic, "Random high-Q cavities in disordered photonic crystal waveguides," Appl. Phys. Lett. **91**(20), 201102 (2007).
28. A. Taflove, and S. C. Hagness, Computational Electrodynamics–The Finite-Difference Time Domain Method (Artech House, 2005).
29. E. Kuramochi, M. Notomi, S. Hughes, A. Shinya, T. Watanabe, and L. Ramunno, "Disorder-induced scattering loss of line-defect waveguides in photonic crystal slabs," Phys. Rev. B **72**(16), 161318 (2005).
30. A. Parini, P. Hamel, A. De Rossi, S. Combrié, N.-V.-Q. Tran, Y. Gottesman, R. Gabet, A. Tanleau, Y. Jaouën, and G. Vadalà, "Time-wavelength reflectance maps of photonic crystal wavegudes: A new view on disorder-induces scattering," J. Lightwave Technol. **26**(23), 3794–3802 (2008).
31. L. O'Faolain, T. P. White, D. O'Brien, X. Yuan, M. D. Settle, and T. F. Krauss, "Dependence of extrinsic loss on group velocity in photonic crystal waveguides," Opt. Express **15**(20), 13129–13138 (2007).
32. K. Srinivasan, and O. Painter, "Momentum space design of high-Q photonic crystal optical cavities," Opt. Express **10**(15), 670–684 (2002).
33. M. Settle, M. Salib, A. Michaeli, and T. F. Krauss, "Low loss silicon on insulator photonic crystal waveguides made by 193nm optical lithography," Opt. Express **14**(6), 2440–2445 (2006).
34. A. Yariv, Optical Electronics. (Saunders College Publishing, 1991).
35. T. Asano, B. S. Song, and S. Noda, "Analysis of the experimental Q factors (~ 1 million) of photonic crystal nanocavities," Opt. Express **14**(5), 1996–2002 (2006).
36. A. Kuramochi, M. Notomi, S. Mitsugi, A. Shinya, T. Tanabe, and T. Watanabe, "Ultrahigh-Q photonic crystal nanocavities realized by the local width modulation of a line defect," Appl. Phys. Lett. **88**(4), 041112 (2006).
37. C. Manolatou, M. J. Khan, S. Fan, P. R. Villeneuve, H. A. Haus, and J. D. Joannopoulos, "Coupling of modes analysis of resonant channel add-drop filters," IEEE J. Quantum Electron. **35**(9), 1322–1331 (1999).
38. E. Waks, and J. Vuckovic, "Coupled mode theory for photonic crystal cavity-waveguide interaction," Opt. Express **13**(13), 5064–5073 (2005).

1. Introduction

Two-dimensional (2D) photonic crystals (PhCs) in dielectric slabs [1,2] have attracted considerable interest due to their ability to slow-down and confine light it in small spaces. Slow-light propagation and localization are advantageous for a variety of photonic applications. They enhance the strength of interactions between radiation and matter which can facilitate detection and utilization of nonlinear [3–5] and quantum effects [6,7]. PhC-based nanoscale resonators and waveguides are poised to play a crucial role in future miniaturized photonic devices such as nanocavity lasers [8], single photon sources [9], compact filters [10], all-optical switches [11,12], delay lines [13], and refractometric sensors [14]. Structural disorder limits the performance and the capabilities of these devices.

Implications of structural disorder have been very well studied [15–19]. Most of the work focused on in-plane disorder which breaks the periodicity of the 2D photonic lattice causing the optical waves propagating in intrinsically lossless photonic crystal waveguides (PhCWs) to scatter. Disorder-induced back- and out-of-plane scattering have been shown to be the

#109000 - $15.00 USD Received 20 Mar 2009; revised 17 Jun 2009; accepted 30 Jun 2009; published 8 Jul 2009

dominant losses in the important slow-light regime [17]. Interesting disorder-induced localization effects that affect wave propagation have also been reported in this regime in coupled-resonator chains [20], disordered 1D lattices [21], and line-defect PhCWs [22,23]. Vertical (or out-of-plane) asymmetry is another significant but far less studied contributor to the guiding losses. While several loss channels related to polarization conversion have been identified and observed experimentally [24–26], the effects of intermodal interactions in dispersive waveguides and their contributions to out-of-plane losses have not yet been sufficiently studied.

In this article we investigate vertical scattering in disordered PhCWs composed of lines of voids in 2D photonic lattices in free-standing silicon slabs. The fabricated PhCs contain enhanced in-plane disorder created by random orientations of non-circular lattice elements, and their out-of-plane symmetry is also perturbed by a sidewall tilt. We study how these structural asymmetries affect propagation of linearly polarized light through the dispersive waveguides. Our study highlights the spectrally narrow enhancement of polarization conversion associated with band edge intermittency due to disorder. Finally, we also introduce a mechanism based on polarization-mixing for coupling light into PhC-based resonators, demonstrating that TE-like high-Q nanocavities in vertically asymmetric PhCWs can be excited with TM-like guided modes.

2. Fabrication of disordered waveguides and experimental setup

PhC slabs were fabricated on silicon-on-insulator (SOI) substrates using electron-beam lithography and reactive ion etching (RIE). PhC waveguides (also known as W1) were defined in a triangular array of air-holes by a line of voids along the Γ-K reciprocal lattice direction. The in-plane cross-sections of the etched holes are not perfectly circular and their sidewalls deviate from the vertical by a tilt angle θ~4° as shown schematically in Fig. 1(a). The shape disorder perturbs the in-plane regularity of the 2D dielectric lattice which leads to modulation of local density of states, and the sidewall tilt is a perturbation causing polarization mixing between TE- and TM-like modes [24]. Both imperfections are common in fabricated PhCs, but in the study described here the magnitude of these irregularities is manipulated to amplify effects of structural disorder. In particular, the RIE process was adjusted to produce moderately slanted sidewalls and in-plane disorder was enhanced by creating arrays of regularly spaced but randomly oriented holes with non-circular (polygonal and elliptical) cross-sections [27]. Scanning electron microscope (SEM) images of typical fabricated PhCWs embedded in a periodic array of randomly oriented ellipses and hexagons, and the cleaved edge showing the tilt are presented in Figs. 1(b) and 1(c), respectively. The design parameters of the underlying periodic crystal with orientational disorder were chosen so that the modal cutoff of the laterally even TE-like guided mode falls within the tuning range of the external cavity laser (1475-–1580nm tunability, 100kHz linewidth, 1pm spectral resolution, 14dB polarization extinction ratio) used in subsequent measurements. This was achieved with the slab-thickness h≈220nm and ~30% air-fill-factor of the lattice. Waveguides with different lattice constants, a = 400, 405, and 410nm, were fabricated with both types of structural disorder (hexagons and ellipses) to offset possible variations of the lattice fill-factor which could shift the TE-like mode-edge out of the available tuning range.

#109000 - $15.00 USD Received 20 Mar 2009; revised 17 Jun 2009; accepted 30 Jun 2009; published 8 Jul 2009

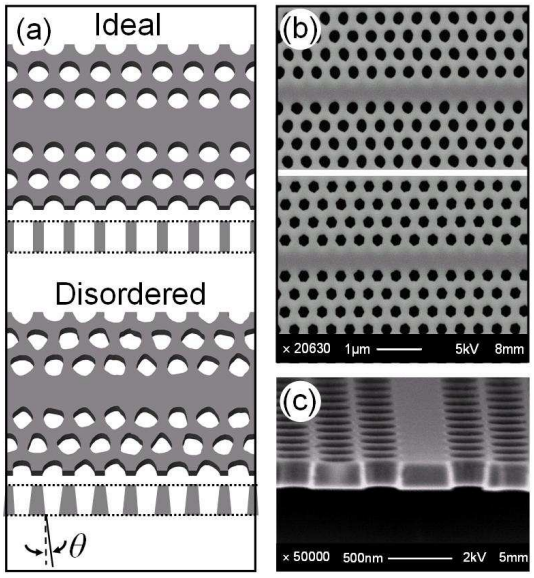

Fig. 1. (a) Schematic of an ideal PhCW formed by a line of voids along in a triangular lattice of air-holes (left) and a disordered structure with broken in-plane (shape variations) and out-of-plane (sidewall tilt) symmetries, (b) top SEM image of a fabricated disordered waveguides composed or randomly oriented ellipses (top) and hexagons (bottom), and (c) vertical cross-section showing the sidewall tilt.

Optical wave propagation through the disordered waveguides was studied by monitoring light scattered vertically out of the PhC slabs. The measurement setup is shown schematically in Fig. 2(a). A fiber-optic polarization controller was used to adjust the polarization state of the probing light which was then coupled into the PhCWs from a tapered single-mode optical fiber (SMF-28) aligned with the line of voids as illustrated in Fig. 2(b). The measured pre-coupling polarization extinction ratio was only ~10dB (significantly smaller than that of the laser source (14dB)) which is likely caused by slight asymmetries of the conical taper prepared by melting and stretching an optical fiber. Radiation emitted vertically out of the PhC plane was collected with a large numerical aperture (NA = 0.8) objective and detected with an InGaAs photodiode as well as a near-infrared imaging camera. A broad-band polarizer positioned in front of the photodetector was used to measure polarization of the vertically-scattered light. To reduce signal noise, the laser source was amplitude modulated at 1kHz and the photocurrent from the diode was amplified with a lock-in amplifier referenced to the modulation frequency. The amplifier output was recorded and plotted against the probing wavelength. Simultaneously, the out-of-plane emission was also imaged while the laser was tuned through the spectral range around the TE-like guided-mode cutoff. Integrated scattering intensity profiles along the waveguide axis were also plotted against the probing wavelength. This experimental modality ensured unambiguous determination of the spectral linewidths, sizes, positions and polarizations of the sources of the collected light. The marked peaks in the detected surface emission intensity are shown schematically in Fig. 2(b). They correspond to the enhanced vertical scattering at the PhCW input (Peak 1), inside the disordered waveguide (Peak 2), at the output (Peak 3), and at the other facet of the cleaved SOI wafer (Peak 4). The scattering spot at the waveguide output is produced in part by photonic surface states formed at the lattice termination and by the light transmitted through the waveguide which is reflected towards the output from the cleaved facet. A fraction of this reflected light then scatters off the tapered etched holes towards the photodiode. The intensity of this scattering spot thus provides indirect qualitative information about transmission through the structure.

#109000 - $15.00 USD Received 20 Mar 2009; revised 17 Jun 2009; accepted 30 Jun 2009; published 8 Jul 2009

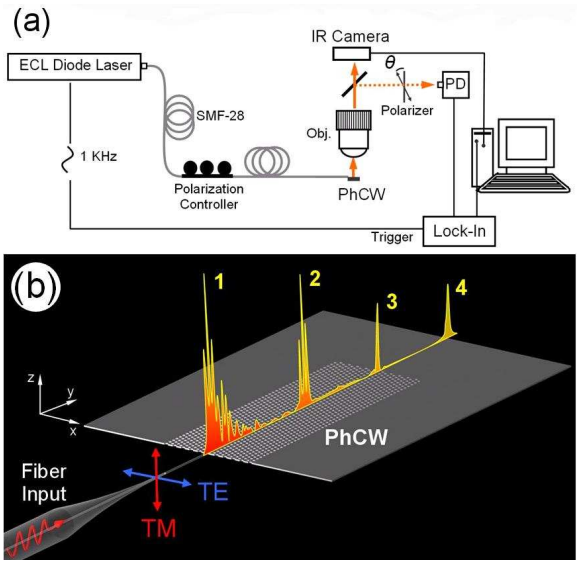

Fig. 2. (a) Schematic of the experimental setup. Light output from a tunable external cavity laser (ECL) was coupled into PhCWs from silica fiber taper and vertically-scattered light was analyzed with a photodiode (PD) and an infrared (IR) Camera. (b) Detailed representation of the employed coupling scheme. Marked scattering features in the surface emission (orange peaks) represent the scattered light intensity: (1) at the input facet, (2) inside the waveguide, (3) at the waveguide output, and (4) at the cleaved facet. The blue and red arrows mark the electric-field vector orientation the TE and TM polarizations.

3. Optical wave transport characterization

Light transport in PhCWs is strongly polarization dependent. The difference is highlighted in the band diagrams of the TE- and TM-like modes presented in Fig. 3. The band structure of an ideal W1 in a perfect PhC lattice composed of cylindrical air-holes was calculated using finite-difference time-domain (FDTD) technique [28]. TE-polarized light is guided along the line of voids by total internal reflections (index guiding) in the plane of the membrane and by Bragg reflections in the transverse direction. W1 supports multiple TE-like guided modes within the bandgap, but we only investigate a narrow band at $\omega\cong 0.260–0.275[a/\lambda]$ ($\lambda\cong 1473–1557$nm) where the TE-like waveguiding is single-mode. Two distinct propagation regimes, *viz.* index guiding and photonic bandgap (or slow-light) guiding can be classified via the dispersion diagram in Fig. 3(a). In the index-guiding regime (black circles) the light is guided by a laterally even TE-like mode with a large group velocity ($v_g = d\omega/dk$) and is mostly unaffected by structural disorder. In the slow-light regime (gray circles) on the other hand, the waves propagate with a small group velocity which decreases gradually as the wavelength approaches the edge of the stop-band at $\omega\cong 0.264[a/\lambda]$ ($\lambda\cong 1534$nm). The combination of slow-light conditions and structural disorder is known to cause out-of-plane and backscattering losses even if the guided modes are below the light-line [17].

Typical spatially-resolved spectra of the vertical emission measured for the two probing polarizations are shown in Fig. 4(a). The horizontal axis represents the excitation wavelength and the vertical axis the position along the disordered W1 composed of a 2D triangular array (a = 405nm) of randomly oriented hexagons shown in Fig. 1(b). Probing light is incident from the bottom of the 2D plots where the high measured intensity is produced by scattering at the input (Peak 1 in Fig. 2(b)) and the bright line at 140μm-vertical marks the waveguide's end (Peak 3). This light carries the polarization signature of the transmitted light as it is polarized primarily along the waveguide axis for the TM and perpendicular to it for the TE excitation. The polarization extinction ratio of the output spot varies for the two cases with the tuning wavelength but it remains fairly constant at ~8dB below 1510nm where both modes are index-

#109000 - $15.00 USD Received 20 Mar 2009; revised 17 Jun 2009; accepted 30 Jun 2009; published 8 Jul 2009

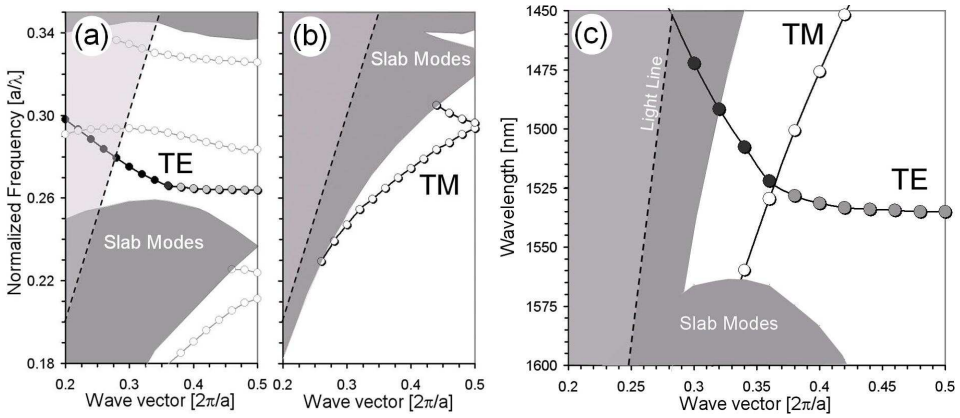

Fig. 3. (a) Calculated band diagrams of the underlying periodic crystal for the TE-like and (b) TM-like guided modes. (c) Detailed image of the band structure around the TE-like mode-edge showing both TE- and TM-like guided modes.

guided. All the other sources of vertical emission observed along the waveguide are produced presumably by structural disorder. Spatial distribution of these scattering features is markedly different for the two probing polarizations. TE-polarized light excites both spectrally broad, spatially extended sources which span over the full length of the waveguide and narrow-linewidth, point-like sources positioned in the proximity of the input facet. On the other hand, the features excited with TM polarization are spectrally and spatially narrow, and they are distributed throughout the disordered waveguide.

The features produced by excitation with TE-polarized light can be explained with disorder-induced backscattering and out-of-plane scattering in dispersive PhCWs. Ideally, the only available propagation channels are forward and backward directions along the line of voids. Transverse leakage is prohibited by photonic bandgap and out-of-plane leakage is prevented by total internal reflections since the mode is below the light-line. PhCWs are known to be rather immune to structural imperfections when operated in the index-guided regime, but they suffer significant losses in the slow-light regime. These are generally attributed to nanometer-scale surface roughness that causes a gradual increase of scattering at wavelengths approaching the stop-band boundary. Theoretical analysis predicts simple scaling of the out-of-plane and backscattering losses with the inverse of the group velocity and the inverse of the group velocity squared, respectively [17]. The scaling laws generally hold for state-of-the-art waveguides with minimal residual disorder [29], but in presence of more severe imperfections disorder-induced backscattering causes a severe intermittency of the mode-edge which gives rise to slowly-guided and localized resonant states [22,27,30,31].

Our experiments show that the investigated W1 with enhanced in-plane disorder exhibits nearly ideal waveguiding behavior at wavelengths below 1510nm where we find no apparent vertical leakage and the intensity of the scattering spot at the waveguide output indicating overall transmission (140μm horizontal in Fig. 4(a)) remains uniform. At longer wavelengths, we observe an onset of vertical scattering accompanied by a commensurate reduction of the transmitted intensity. The scattering intensity does increase with the probing wavelength gradually on average, but it also exhibits narrow-band fluctuations. Light propagation is often suppressed significantly by disorder-induced stop-bands, in which case the scattering spot at the waveguide output almost vanishes, or it is allowed via extended resonant states. Both possibilities can be clearly observed in Fig. 4(c) in the spectral region from 1524.0nm up to 1526.3nm. At 1526.3nm, there is an abrupt drop in the transmission which effectively corresponds to the modal cutoff of the disordered waveguide. Beyond this cutoff, the spatially resolved scattering spectra show signs of localization in the form of spectrally-narrow, high-intensity peaks positioned inside the disordered waveguide. These resonances can be excited

#109000 - $15.00 USD Received 20 Mar 2009; revised 17 Jun 2009; accepted 30 Jun 2009; published 8 Jul 2009

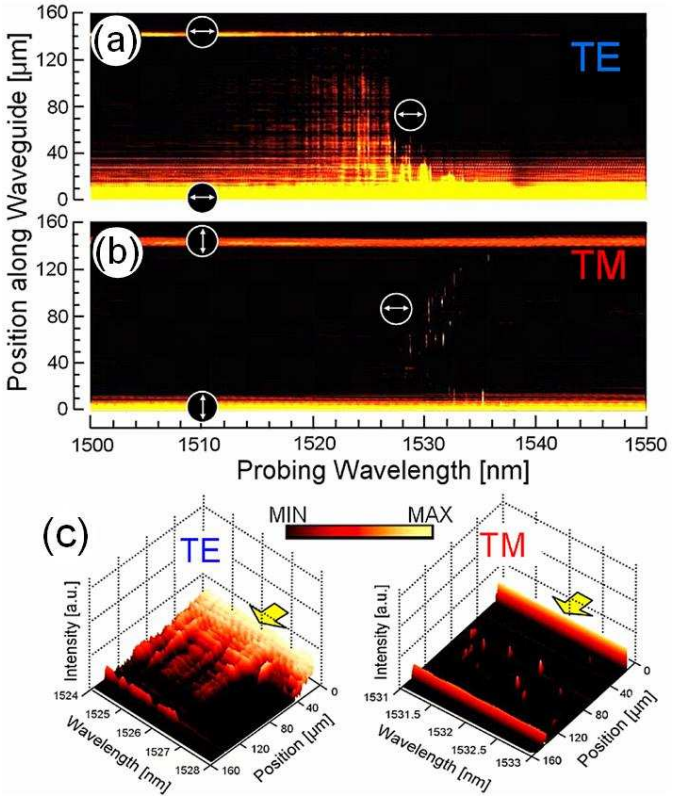

Fig. 4. (a) Spatially resolved spectra of the vertically-emitted light measured for the TE- (a) and TM-polarization (b). The light is incident from the bottom of the figures and the arrows indicate polarization direction of the detected light. (c) Detailed scans of the scattering features obtained for both polarizations.

by evanescent coupling, but only if they are positioned sufficiently close to the waveguide input. One of such isolated features appears for example at 1527nm as seen in Fig. 4(c). In-plane polarization analysis of these spectral peaks revealed that they are *all* polarized primarily (with ~6dB extinction ratio) in the direction orthogonal to the waveguide axis. Spatially localized states in PhC slabs are intrinsically leaky because the vertical confinement is provided by incomplete total internal reflections. Fourier transforms of their field intensities always contain *k*-vector components that are not internally reflected and can leak vertically out of the slab [32]. Note that since we only monitored vertical leakage in the far-field, not the field intensities inside the waveguide, we are unable to measure the field envelopes needed to unambiguously confirm formation of localized states with exponentially decaying field profiles. With this experiment we therefore cannot distinguish out-of-plane emission caused by extrinsic losses such as dispersive slow-light scattering (and polarization scattering discussed in the next section) from emission through localized states. We believe the two effects coexist in the investigated spectral region and are both contributing to the observed scattering features.

TM-polarized light propagates along lines of voids in PhC slabs classically by index-guiding in both lateral and vertical directions. Calculated dispersion diagram in Fig. 3(b) shows the fundamental TM-like mode associated with guiding. The mode has a large group velocity in the probed wavelength range and it is below both the light-line and the continuum of laterally extended TM-like slab modes. No significant transverse or out-of-plane leakage due to slow-light effects or coupling to leaky mode-edge defects is therefore anticipated. Our measurements of vertical losses are consistent with these expectations in that they show stable

#109000 - $15.00 USD Received 20 Mar 2009; revised 17 Jun 2009; accepted 30 Jun 2009; published 8 Jul 2009

intensity of the scattering spot at the waveguide's output and virtually no gradual increase of out-of-plane scattering. However, a band of spatially isolated and spectrally sharp emission peaks with $\lambda/\Delta\lambda$ of over 600,000 is also observed at wavelengths between 1528nm and 1539nm, in the same range where similar patterns were detected in the proximity of the input facet when TE-polarized light was coupled into the waveguide. Figure 4(c) is a detailed spatial-frequency map of the scattering features. Unlike the sources of vertical emission probed with TE light, many of those excited with TM-polarization appear far from the input facet. They exhibit narrow linewidths and are polarized perpendicular to the waveguide axis (with ~6dB extinction ratio), i.e. they are TE-like. That observed polarization is orthogonal to the polarization of the scattering spot at the waveguide output generated by the transmitted light. From this we conclude that polarization conversion takes place in the disordered waveguide.

Experimental evidence of polarization-mixing between the fundamental TE- and TM-like modes guided below the light-line in vertically asymmetric PhCWs has been observed in the transmission [25,33] and reflection spectra [30]. The conversion can be explained within the framework of traditional coupled-mode theory by counter-directional coupling which arises when the two modes coincide in the momentum-frequency plane [34]. This occurs in our W1 waveguide at $\omega \cong 0.2656[a/\lambda]$ ($\lambda \cong 1525$nm) as can be seen in the calculated dispersion diagram in Fig. 3(c). Spectral proximity of this crossing to the TE-like modal cutoff suggests that coherent interactions between the two counter-propagating modes could be involved in the formation of the narrow spectral features observed in our measurements. In-plane disorder plays two distinct roles in the proposed process. Firstly, it provides lateral asymmetry necessary for the TE-TM coupling. Parity considerations reveal that the two orthogonal fundamental modes interact only if both vertical and transverse symmetries with respect to the propagation axis are broken by perturbation. Secondly, the in-plane disorder creates TE-like mode-edge resonances which can spectrally overlap with the mini-stopband formed by anti-crossing of TE- and TM-like guided modes. The isolated peaks observed in the surface emission between 1528nm and 1539nm could thus be explained by resonant polarization scattering from the TM-like guided mode into spectrally distinct TE-like slow-light modes generated by disorder. If such a mechanism is responsible for the formation of the features, their narrow spectral linewidths would not necessarily indicate long photon lifetimes (or high Qs) of disorder-induced random cavities, but could instead reflect the resonant nature of the polarization conversion.

4. Excitation of PhC nanocavities by polarization mixing

Another coupling scenario with a different vertical scattering signature can be expected at frequencies inside the TE-like stop-band where the TE-like waveguiding is prohibited, but the underlying crystal can nevertheless support spatially-localized, long-lived defect modes (or high-Q PhC cavities). TM-polarized light is allowed to propagate along the waveguide and the fundamental TM-like mode could thus serve as an independent channel for delivering light into these cavities. In this case, the spectral linewidths measured in the out-of-plane emission would indeed be an indicator of the total cavity Qs. Although it is conceivable that such localized modes exist in the deliberately disordered W1 waveguides, our experimental method lacks the spatial resolution necessary to corroborate this. Also, for reasons discussed earlier, we cannot use the spectral information to conclude that isolated high Qs nanocavities are created by disorder.

To investigate the possibility of the waveguide-cavity coupling based on polarization-mixing more accurately and without doubts that a cavity exists near the waveguide, we created an engineered localized state inside the TE-like stop-band by fabricating a PhC heterostructure nanocavity similar to those studied by Asano *et al*. [35] and Kuramochi *et al*. [36]. Our cavity was formed by shifting several circular air-holes laterally and along the waveguide. The surrounding photonic lattice contains no enhanced in-plane disorder other than the imperfections introduced during fabrication. Lattice constants of the individual PhC sections are: a_1 = 400nm, a_2 = 405nm, a_3 = 410nm as shown schematically in Fig. 5(a). The

#109000 - $15.00 USD Received 20 Mar 2009; revised 17 Jun 2009; accepted 30 Jun 2009; published 8 Jul 2009

calculated electric-field profile of the cavity mode with a small modal volume of ~$1.3(\lambda/n)^3$ is presented in Fig. 6(a). PhC-based cavities of this type are traditionally excited by evanescent

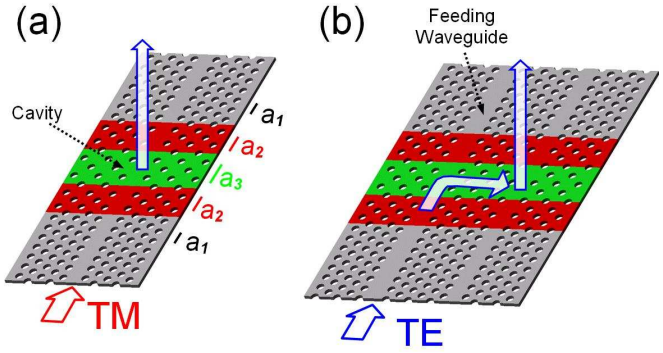

Fig. 5. (a) Schematic of coupling into a PhC heterostructure nanocavity formed by shifting air-holes to locally increase the lattice constant, (b) traditional excitation mechanism based on evanescent coupling from an adjacent feeding waveguide.

coupling of TE-polarized light from an adjacent feeding waveguide [35,36] as shown in Fig. 5(b). In this configuration, the coupling strength can be controlled by changing the distance between the cavity and the feeding waveguide. In our measurements, on the other hand, TM-polarized light was coupled directly into the waveguide with broken out-of-plane symmetry (sidewall tilt) in which the resonator resides (see Fig. 5(a)). The observed defect resonance is shown in the high-resolution spectra and the spatially-resolved spectra in Fig. 6(b) and 6(c), respectively. Its experimental Q of ~94,000 is comparable to the experimental values measured in similarly designed PhC nanoresonators excited by evanescent coupling [36].

The alternative excitation mechanism explored here can be explained with coupled-mode theory as coupling between optical resonators and waveguides [37,38]. The case at hand can be treated as an interaction between a standing-wave resonator and a non-dispersive waveguide which forms the basis of optical add-drop filters. Although not discussed at this time in further detail, preliminary 3D FDTD simulations show that excitation of the laterally symmetric TE-like cavity mode shown in Fig. 6(a) by direct coupling from the TM-like guided mode is extremely inefficient even if relatively large sidewall tilts of up to 15° are introduced. This can be understood by recognizing that coupling between TM- and TE-like modes in a disorder-free W1 is possible only if the transverse symmetry of the cavity-waveguide system is broken, which follows directly from parity considerations. Weak asymmetries are created in real structures by fabrication disorder making excitation of high-Q cavity modes essentially always possible, but the efficiency of energy transfer is expected to be very low even though the cavity and the waveguide overlap spatially. Coupling can be improved by deliberately enhancing the vertical and transverse asymmetries of the nanocavities which would however degrade their Qs by increasing the vertical radiation losses. Adjustments of the level of asymmetry can achieve a balance between coupling efficiency and spectral purity appropriate for the particular application. Since vertical asymmetry required for polarization-mixing in free standing PhC slabs is also a major factor contributing to the degradation of the cavity Q [35], the implementation of the scheme would likely reduce the spectral selectivity of the cavity-waveguide system. Increasing the cavity asymmetry in the polarization-mixing scheme is analogous to reducing the separation between the waveguide and the cavity in the evanescent side-coupling scheme. More studies are needed to determine how the two approaches compare quantitatively. Nevertheless, by eliminating the need for an additional input waveguide, the introduced coupling mechanism could be very convenient for large-scale optical integration of cavities and waveguides on intrinsically asymmetric photonic platforms such as SOI.

#109000 - $15.00 USD Received 20 Mar 2009; revised 17 Jun 2009; accepted 30 Jun 2009; published 8 Jul 2009

It is interesting that in addition to the isolated resonance at $\lambda \cong 1494.75$nm supported by the designed nanocavity, spatially and spectrally distinct scattering features distributed along the waveguide were also observed at shorter wavelengths as can be seen in Fig. 6(c). Surprisingly, their linewidths are comparable to that of the engineered high-Q cavity mode even though the PhC contains no enhanced disorder that could explain formation of isolated deep-level defects. We thus suspect that these spectrally narrow band-edge features do not indicate large Qs of some localized states but are the consequence of residual disorder enhancing the polarization scattering into extended quasi-states. This also appears to be a more likely explanation for the sharp spectral peaks observed in the deliberately disordered waveguides. Additional studies are being conducted to conclusively confirm this.

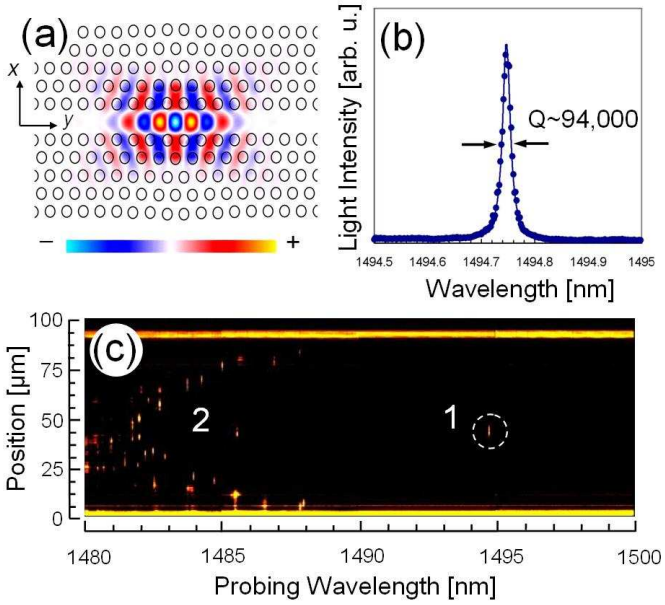

Fig. 6. (a) Calculated mode profile showing the *x*-component of the electric field, (b) measured vertically-scattered spectra showing a high-Q resonance supported by the point-defect, and (c) spatially-resolved spectra showing spectrally isolated engineered cavity resonance (1) and a band of random mode-edge resonances (2).

5. Conclusions

In conclusion, we have characterized the band-edge and disorder enhanced polarization conversion in vertically asymmetric PhC-based slab waveguides. Both measurements and simulations indicate that while longitudinal disorder largely determines the intermittency of the mode-edge, it is the transverse and vertical asymmetries that are necessary for polarization conversion in this system. Furthermore, we have verified that this polarization conversion is enhanced by narrow spectral features at the band edge. Nevertheless, the present data indicates that the spectral linewidths cannot be used to reliably assess the quality of photon confinement in disordered W1 waveguides. We have also introduced a mechanism for PhC nanocavity excitation based on TM-TE polarization mixing in vertically asymmetric slabs. The presented findings could be interesting for applications of PhC cavities and waveguides in optical signal processing and ultra-sensitive refractometric sensing.

Acknowledgements

This work was supported by the Rowland Junior Fellowship program and was performed in part at the Cornell NanoScale Facility and the Center for Nanoscale Systems, members of the National Nanotechnology Infrastructure Network, which is supported by the National Science Foundation (Grant ECS-0335765). M. C. acknowledges additional support through a

#109000 - $15.00 USD Received 20 Mar 2009; revised 17 Jun 2009; accepted 30 Jun 2009; published 8 Jul 2009

Radcliffe Institute for Advanced Studies Fellowship. J. T. acknowledges Zao Liu for useful discussions and help with FDTD simulations.

#109000 - $15.00 USD Received 20 Mar 2009; revised 17 Jun 2009; accepted 30 Jun 2009; published 8 Jul 2009